CORA Cork Open Research Archive
Cartlann Taighde Oscailte Chorcaí

Title	Electrochemical pore formation on InP in alkaline solutions
Authors	Harvey, E.;O'Dwyer, Colm;Melly, T.;Buckley, D. Noel;Cunnane, V. J.;Sutton, David;Newcomb, Simon B.;Chu, S. N. G.
Publication date	2001-09-01
Original Citation	Harvey, E., O' Dwyer, C., Melly, T., Buckley, D. N., Cunnane, V. J., Sutton, D., Newcomb, S. B. and Chu, S. N. G. (2001) 'Electrochemical Pore Formation on InP in Alkaline Solutions', State-of-the-Art Program on Compound Semiconductors XXXV, 200th Meeting of the Electrochemical Society , 2-9 September, San Francisco, California, in Proceedings - Electrochemical Society, Vol. 20, pp. 87-95. ISBN 1566773539
Type of publication	Article (peer-reviewed)
Link to publisher's version	http://ecsdl.org/site/misc/proceedings_volumes.xhtml
Rights	© 2001, Electrochemical Society
Download date	2026-11-06 14:53:19
Item downloaded from	https://hdl.handle.net/10468/2884

UCC
University College Cork, Ireland
Coláiste na hOllscoile Corcaigh

ELECTROCHEMICAL PORE FORMATION ON InP IN ALKALINE SOLUTIONS

E. Harvey[1,2], C. O'Dwyer[1,2], T. Melly[1,2], D.N. Buckley[1,2],
V.J. Cunnane[1,3], D. Sutton[1], S. B. Newcomb[1], and S.N.G. Chu[4]

[1] Materials and Surface Science Institute, University of Limerick, Ireland
[2] Dept. of Physics, University of Limerick, Ireland
[3] Dept. of Chemistry and Environmental Science, University of Limerick , Ireland
[4]Agere Systems, Murray Hill, N.J., U.S.A.

ABSTRACT

The surface properties of InP electrodes were examined following anodization in $(NH_4)_2S$ and KOH electrolytes. In both solutions, the observation of current peaks in the cyclic voltammetric curves was attributed to selective etching of the substrate and a film formation process. AFM images of samples anodized in the sulfide solution, revealed surface pitting and TEM micrographs revealed the porous nature of the film formed on top of the pitted substrate. After anodization in the KOH electrolyte, TEM images revealed that a porous layer extending 500 nm into the substrate had been formed. Analysis of the composition of the anodic products indicates the presence of In_2S_3 in films grown in $(NH_4)_2S$ and an In_2O_3 phase within the porous network formed in KOH.

INTRODUCTION

Semiconductor structures with nanometer scale dimensions can result in drastic changes in the electrical and optical properties relative to those of the bulk material. Anodization of Si in fluoride containing electrolytes has been studied extensively [1-3]. It has been found that depending on experimental conditions the pores formed can be classified according to their size as nanopores, mesopores (2-50 nm) and macropores [4]. Since the discovery of strong luminescence from porous Si, other semiconductors have been made porous by electrochemical methods. However, investigation of the conditions resulting in such pore formation in III-V semiconductors and the resulting properties of such layers, is still in its infancy. Opinions differ as to whether new luminescent properties observed in the PL spectra of porous GaAs and GaP are due to quantum confinement effects or a result of anodically formed oxides [5-8]. Both blue and red shifts have been observed in the PL spectra of InP and shifts to sub-bandgap wavelengths are thought to result from quantum confinement effects while red shifts are attributed to surface states induced in the pore walls [9,10]. There have been several reports of the formation of porous structures in InP by anodization in acidic solutions, in particular HCl. In this paper we report on anodic pore formation in InP in alkaline solutions (KOH and $(NH_4)_2S$).

EXPERIMENTAL

The InP (100) wafers were n-type with carrier concentrations in the range 2-5 x 10^{18} cm^{-3}. Two alkaline electrolytes were used: 3 mol dm^{-3} aqueous $(NH_4)_2S$ and 5 mol dm^{-3} KOH. Indium was alloyed to the InP samples to form the ohmic contact and the contact was insulated from the electrolyte by coating with a varnish. A three electrode configuration was used for the electrochemical experiments: the InP working electrode, a Pt counter electrode, and a saturated calomel reference electrode. All potentials are referenced to the saturated calomel electrode (SCE). Experiments were carried out at room temperature and in the dark.

For cyclic voltammetric measurements, a CH Instruments Model 650A Electrochemical Workstation was employed for cell parameter control and for data acquisition. The structural properties of the anodized samples were examined by atomic force microscopy (AFM) and transmission electron microscopy (TEM). Electron diffraction and X-ray photoelectron spectroscopy (XPS) were used to identify the composition of the anodic reaction products.

RESULTS AND DISCUSSION

Ammonium sulfide electrolyte

Fig 1. shows cyclic voltammetric measurements of an InP electrode in an $(NH_4)_2S$ electrolyte. The potential was scanned at a rate of 10 mV s^{-1} between an initial value, E_i, of 0.0 V and upper potentials, E_u, of 0.785 V and 0.88 V respectively.

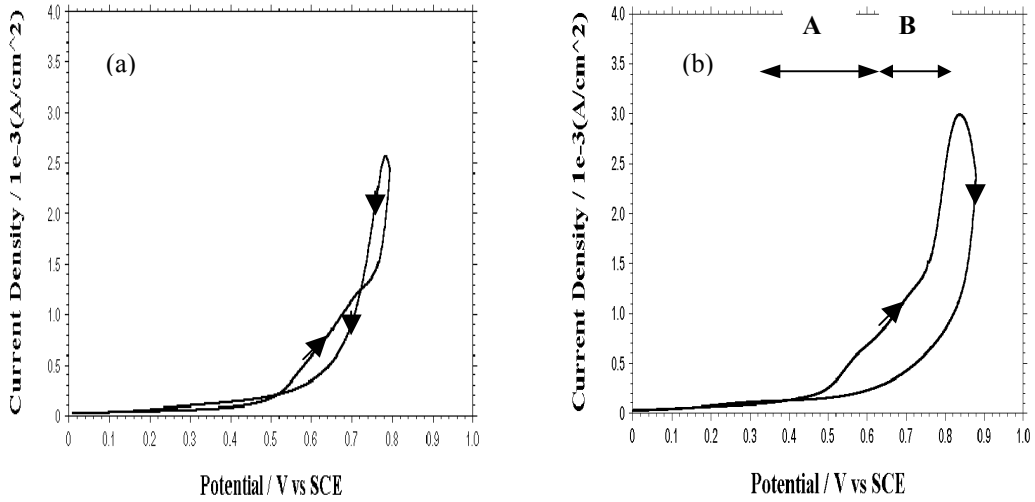


Fig. 1 Cyclic voltammograms of InP in 3 mol dm^{-3} $(NH_4)_2S$ at a scan rate of 10 mV s^{-1}. E_i = 0.0 V; (a) E_U = 0.785 V(SCE) and (b) E_U = 0.88 V(SCE)

It was found that when E_U was less then the peak potential, E_P, the value of the current on the return scan was similar to the corresponding current on the forward scan as can be seen in Fig. 1(a). The current-voltage characteristics obtained when E_U = 0.88 V (i.e. above the peak potential) are shown in Fig. 1(b). In this case the current density on the cathodic scan was considerably lower than on the anodic scan. Such results suggest that the peak in current density corresponds to passivation of the surface by a deposited film which also inhibits current flow on the cathodic scan.

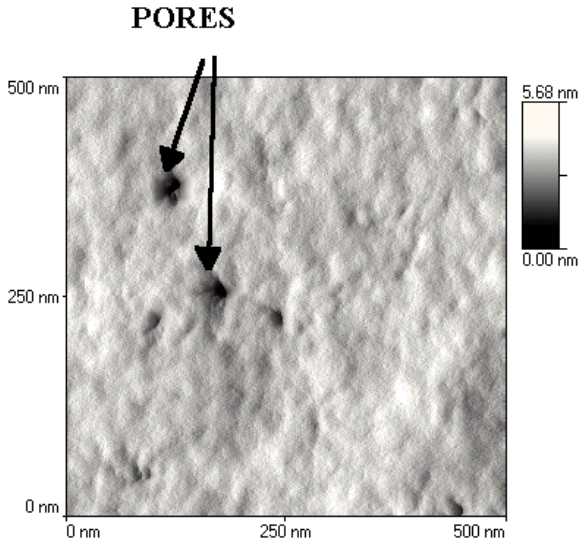
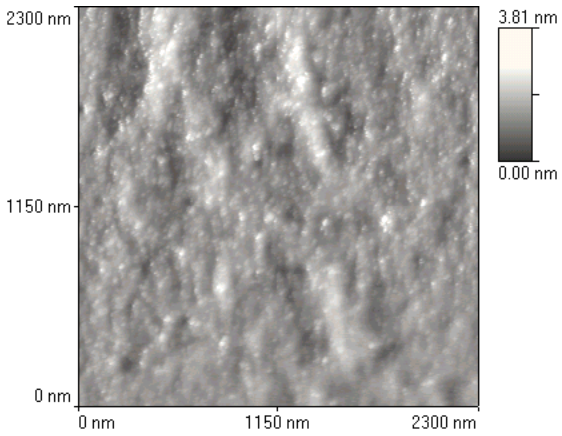


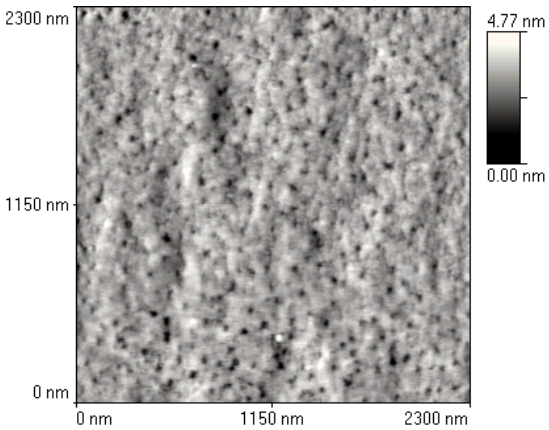
Fig. 2 AFM image of an n- InP sample that was scanned from 0.0 V (SCE) to 0.785 V (SCE) at 10 mV s^1 in a 3 mol dm^{-3} $(NH_4)_2S$ electrolyte.

AFM was used to investigate the topography of the InP electrodes following different anodization procedures. Fig. 2 shows a 500 nm x 500 nm AFM image of a sample that was subjected to a linear sweep from 0.0 V to a value of E_U = 0.785 V. On careful inspection it is observed that small holes or pits are dispersed over the surface of the sample. Larger areas of the same electrode were imaged and these pits were found to exist over the whole surface. This indicates that the current observed in region 'B' of Fig. 1(b) is due to selective etching of the InP substrate. If the potential was also scanned back to 0.0 V, an increase in the pit density was observed. Thus current passed on the return scan may also be attributed to selective etching of the InP electrode.

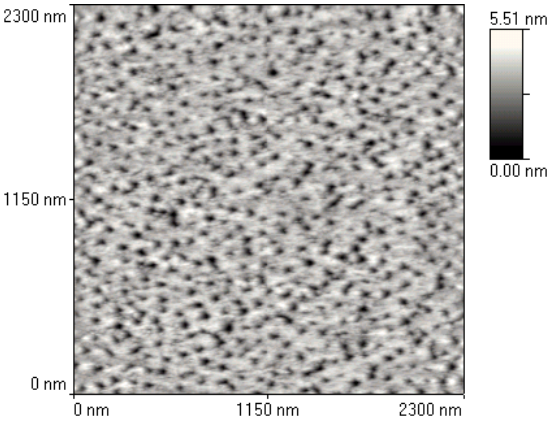
The surface topography was also examined after a sample had undergone anodization up to 0.7 V. However, no pits were observed in the AFM images taken. In order to investigate whether more prolonged treatment would accentuate pore formation, samples were subjected to repeated cycling between 0.0 V and 0.7 V. Even after such treatment, no obvious pits were observed in the AFM images as is



(a)



(b)



(c)

Fig. 3 AFM images showing the surface topography after cyclic voltammogramms from 0.0 V (SCE) up to E_U= (a) 0.7 V (SCE) (b) 0.82 V (SCE) and (c) 0.88 V (SCE) and back to 0.0 V(SCE), in a 3 mol dm^{-3} $(NH_4)_2S$ electrolyte. The image shown in (a) was taken after scanning the potential between 0.0 V and 0.7 V 10 times.

apparent from Fig. 3(a), although the surface was found to have a much rougher texture than that of an untreated electrode. Thus, the onset of pit formation in the InP surface appears to correspond to the rapid rise in current in the potential region indicated as 'B' in Fig. 1(b).

The topography of samples subjected to a potential cycle between 0.0 V and E_U values of 0.82 V (i.e. peak potential) and 0.88 V respectively, were examined. The images are shown in Fig. 3(b) and 3(c) respectively and were taken over an area 2300 nm x 2300 nm. It can be seen in Fig. 3(b) that a surface texture similar to that of Fig. 3(a) is maintained but pits are now also apparent in the image. It is clear from a comparison of Figs. 2, 3(b) and 3(c) that the density of pits continues to increase over the potential range 0.75 V – 0.88 V.

Thus it appears that at potentials between 0.5 V and 0.75 V, etching of the InP occurs with the development of a characteristic surface texture but with no pit formation. Above 0.75 V, pits are formed in the InP surface with a consequent accelerated increase in current. Comparison of AFM images corresponding to potential cycling to 0.82 V and 0.88 V respectively, shows a change in texture probably due to growth of a thicker surface film (35 nm at 0.88 V; see discussion below). The decrease in current following the peak at E_P, and the subsequent reduced current on the reverse scan is indicative of the growth of a passivating film. However, the amount of decrease in current is relatively small, consistent with porosity in the film.

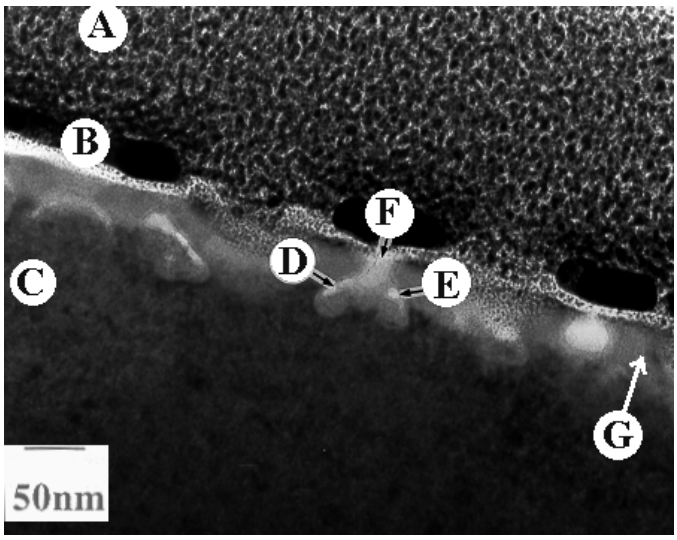


Fig. 4 Cross-sectional TEM image of n-InP after a cyclic voltammetric scan from 0.0 V to 0.88 V and back to 0.0 V in a 3 mol dm^{-3} $(NH_4)_2S$ electrolyte. Labels A and B in this figure indicate Pt and Au coatings respectively, deposited to prevent ion image to the underlying material during the preparation of the TEM sample. The InP substrate is indicated by label C.

TEM images were taken of a cross section of an electrode that had been anodized in a cyclic potential sweep between 0.0 V and 0.88 V: a typical image is shown in Fig. 4. It can be seen that the surface is covered by a film (G), approximately 35 nm in thickness. "Winged" structures are observed which penetrate into the underlying InP substrate. Each of these structures consists of a partially filled pit in the InP with pores ("white wings" at D and E) which connect to a vertical pore (F) in the surface film. The absence of such vertical pores above the winged structure in some cases, is believed to be an experimental artifact due to the TEM slice not passing through the center of each pore. A diffuse dark field image revealed that no crystallites could be observed in the anodic film which appears to be amorphous.

Such winged features of the etched InP are obviously a consequence of the non-uniform etching of the semiconductor electrode. Measurement of the angle between the two wings gives values between 105^0 and 110^0. This corresponds to preferred etching of the semiconductor along the <111> direction. Bright and dark field images of the same surface region were taken. The dark field image illustrates further the accelerated etching along the <111> direction of the InP.

XPS measurements were made of the amorphous film indicated at 'G' in Fig. 4. The energy difference measurements between the S $2p_{3/2}$ peak and the In $3d_{5/2}$ peaks indicates the presence of In_2S_3 [11].

The total charge passed during the cyclic voltammetric scan to 0.88 V was estimated to be 74.5 mC cm^{-2} by integrating the area under the curve. Assuming that this charge corresponds to In_2S_3 formation by an 8-electron process, the film thickness is estimated to be 30 nm, in reasonable agreement with the measured value.

When the potential was increased above 0.88 V, the current was found to increase and then reach a steady state value. It has been reported previously that film growth occurs within this plateau region [12]. TEM images show that film growth is accompanied by further selective etching of the InP substrate. Fig. 5 shows that large pits, typically 150 nm deep, have been etched into the InP surface and an anodic film has been formed, approximately 300 nm in thickness as measured from the outer ends of the pits. The film is columnar in nature with filaments which are observed to be growing from the pits within the InP substrate. Features labeled 'A' in Fig. 5 can be identified as pores within the filaments, and evidence of small crystallites dispersed throughout the columnar film structures was obtained from dark field TEM images. This crystalline phase was identified as In_2S_3 by electron diffraction measurements.

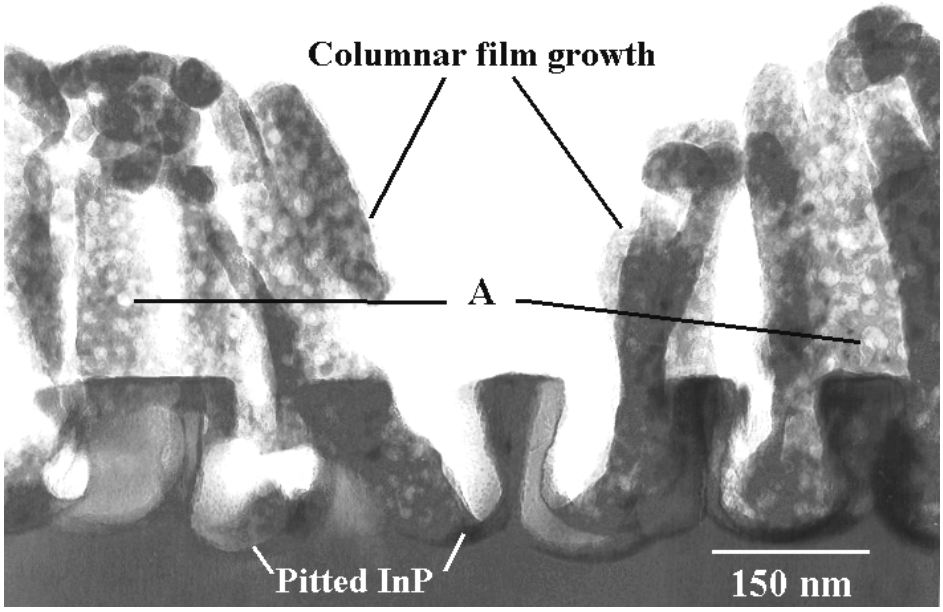


Fig. 5 Cross-section TEM micrograph of a sample anodized in a potential cycle between 0.0 V(SCE) and 1.5 V(SCE) in 3 mol dm^{-3} $(NH_4)_2S$ electrolyte.

Potassium hydroxide electrolyte

Electrochemical measurements were also carried out in a 5 mol dm^3 KOH electrolyte and a peak was observed on the anodic scan as was described previously [13]. The peak in current occurs at 0.48 V and is followed by a current minimum at 0.75 V It was found that the peak current was significantly higher in the KOH solution in comparison to the $(NH_4)_2S$ solution. Fig. 6 shows a cross-sectional TEM image of a sample scanned form 0.0 V up to 0.665 V. It can be seen that anodization in the KOH electrolyte results in a very porous layer being formed within the InP, as indicated by '*A*'. The network of pores extends approximately 500 nm into the substrate, thus accounting for the large current peak observed. Although, in general, pores appear to propagate in a direction perpendicular to the (100) surface of the InP, there is evidence of some branching throughout the porous region. In lower magnification images it is evident that the pores tend to extend into the substrate in a fan-like fashion due to severe branching at the porous layer/ bulk InP boundary. A further noteworthy feature observed in the micrograph is a dense 30-40 nm InP layer which remains at the sample/electrolyte interface and is indicated at '*C*' in Fig. 6.

For pore formation to occur it is necessary that a pathway exists through the upper InP layer (C) that allows contact between the porous region and the electrolyte. TEM images show some evidence of such holes, although their frequency in cross-section is low due to their small size.

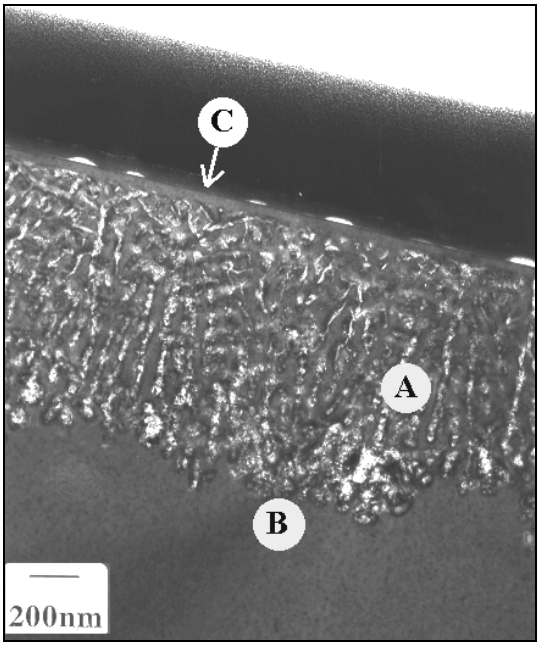


Fig. 6 Cross-sectional TEM image of n-InP after a potential sweep from 0.0 V (SCE) to 0.665 V(SCE) at a scan rate of 2.5 mV s^{-1} in 5 mol dm^{-3} KOH electrolyte. '*B*' denotes the InP substrate.

When the potential was increased above 0.75 V, the current continued to increase with increasing potential. TEM images of the cross sections of a sample subjected to a potential sweep from 0.0 V to 1.45 V indicates that under these conditions of anodization the pore structure has become much coarser and the individual InP segments much smaller. Furthermore the upper InP layer is significantly thinner, measuring only ~20 nm, and the holes in this layer have also become more apparent.

Dark field images of the porous structures confirm the presence of single crystal InP within the porous region and pores appear to be infilled with a reaction product. The ring patterns obtained from electron diffraction measurements indicate the presence of In_2O_3.

It is suggested that the formation of the oxide results initially in a reduction of the current: however increasing the potential above 0.75 V results in a breakdown in the oxide layer which then allows the etching mechanism to continue.

CONCLUSIONS

Two types of surface pitting were observed when InP was anodized in a $(NH_4)_2S$ solution. At lower potentials small pits propagating in the <111> direction in the InP electrode were apparent in the TEM images. In this case a partially porous

film covered the sample after anodization. Potential sweeps to higher potentials (above 0.88 V) resulted in the formation of larger pits. At these higher potentials pit growth was accompanied by the growth of a very porous, columnar type film. In both cases the presence of In_2S_3 in the anodic film was indicated. In contrast, when the semiconductor was anodized in KOH, pores were found to extend deeply into the substrate, resulting in the formation of nanometer-sized InP segments within this porous region. The presence of In_2O_3 within this porous region was detected by electron diffraction measurements.

REFERENCES

(1) P.C. Searson, J. M. Macaulay and F.M. Ross, *J. Appl. Phys.*, **72**, 253 (1992)

(2) T. Osaka, K. Ogasawara and S. Nakahara, *J. Electrochem. Soc.*, **144**, 3226 (1997)

(3) M. Hejjo, A. Rifai, M. Christophersen, S. Ottow, J. Cartensen and H. Foll, *J. Electrochem. Soc.*, **147**, 627 (2000)

(4) V. Lehmann, S. Stengl and A. Luigart, *Mat. Sci. Eng. B,* **69-70**, 11 (2000)

(5) P. Schmuki, L.E. Erickson, D.J. Lockwood, J.W. Fraser, G. Champion and H.J. Labbe, *Appl. Phys. Lett.*, **72**, 1039 (1998)

(6) X. Li and P.W. Bohn, *J. Electrochem. Soc.*, **147**, 1740 (2000)

(7) A. Anedda, A. Serpi, V. A. Tiginyanu, and V. M. Ichizli, *Appl. Phys. Lett.*, **67**, 3316 (1995)

(8) A. Meijerink, A.A. Bol and J.J. Kelly, *Appl. Phys. Lett.,* **69**, 2801 (1996)

(9) T. Takizawa, S. Arai and M. Nakahara, *Jpn. J. Appl. Phys. Pt. 2,* **33**, L643 (1994)

(10) A. Hamamatsu, C. Kaneshiro, H. Fujikura and H. Hasegawa, *J. Electroanal. Chem.*, **473**, 223 (1999)

(11) C.W. Wilmsen, K. M. Geib, J. Shin, R. Iyer, D.L. Lile and J.J. Pouch, *J. Vac. Sci. Technol.*, **B7**, 851 (1989)

(12) E. Harvey, D.N. Buckley, in *Proceedings of the 32nd State-of-the-Art Program on Compound Semiconductors*, R.F. Kopf, A.G. Baca and S.N.G. Chu, Editors, PV 2000-1, p. 265, The Electrochemical Society, Proceedings Series, Pennington, NJ (2000).

(13) E. Harvey, C. O'Dwyer, T. Melly, D.N. Buckley, V.J. Cunnane, D. Sutton, and S.B. Newcomb in *Proceedings of the 34th State-of-the-Art Program on Compound Semiconductors*, F. Ren , D.N. Buckley, S.N.G. Chu, S.J. Pearton, Editors, PV 2001-1, p. 204, The Electrochemical Society, Proceedings Series, Pennington, NJ (2001).